Imaging Metabolomics.

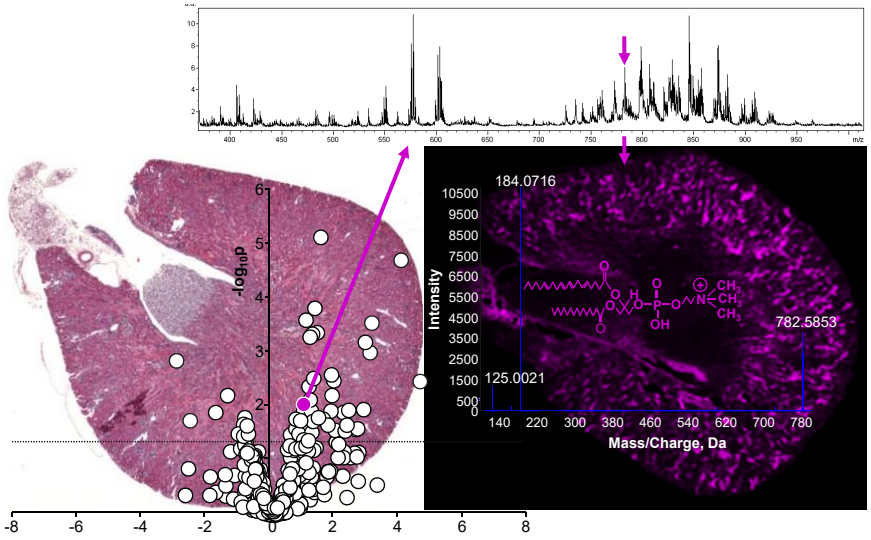

7-27-2018

Janusz Kabarowski, Dept. Microbiology, UAB.

Matrix-Assisted Laser Desorption/Ionization (MALDI):
Matrix molecules absorb laser energy, enter an excited state, and collide with sample molecules, facilitating charge transfer to create ions.

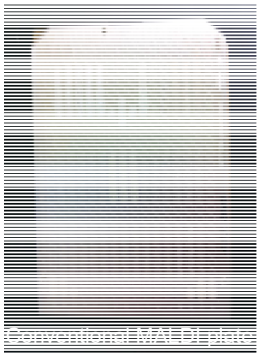

MALDI-TOF instrument

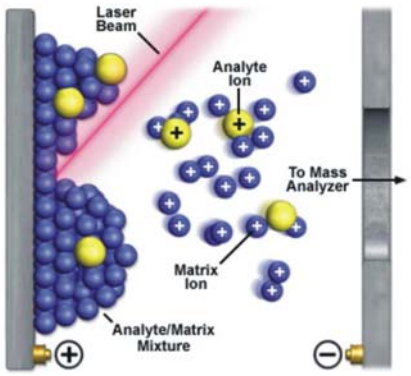

Mass Spectrometric Imaging for biomedical tissue analysis
Kamila Chughtai and Ron M.A. Heeren
Chem Rev. Vol.110(5): pp3237–3277, 2010.

Vacuum sublimation is used to apply an even microscopically thin uniform layer of matrix compound onto tissue section without the need for solvents.

Sublimation: *the transition of a substance from solid to gas phase without an intermediate liquid phase*.

MALDI matrices for lipid imaging:

DHB: 2,5-dihydrobenzoic acid

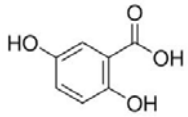

1,5-diaminonapthalene

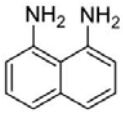

Cryosectioning onto Indium Tin Oxide (ITO) coated glass slides and scanning digital image of slide for "teaching" FlexControl software on MALDI-TOF.

Cryosectioning
2.6% Na carboxymethylcellulose embedded tissue block

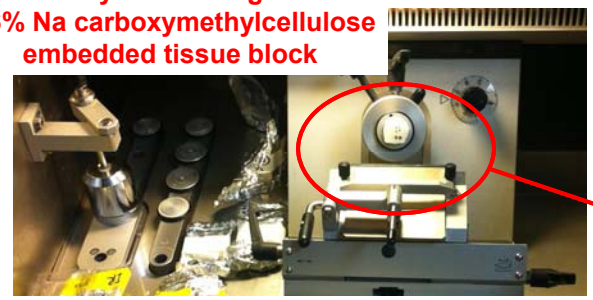

Minimum 2400dpi cryosection image

Matrix application

Vacuum sublimation apparatus for matrix application in MALDI Imaging.

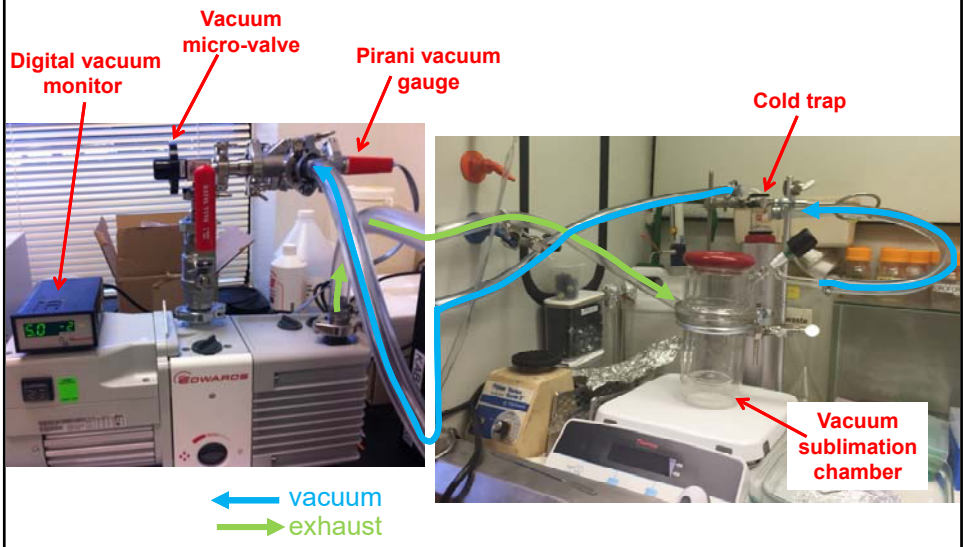

Matrix deposition by vacuum sublimation.

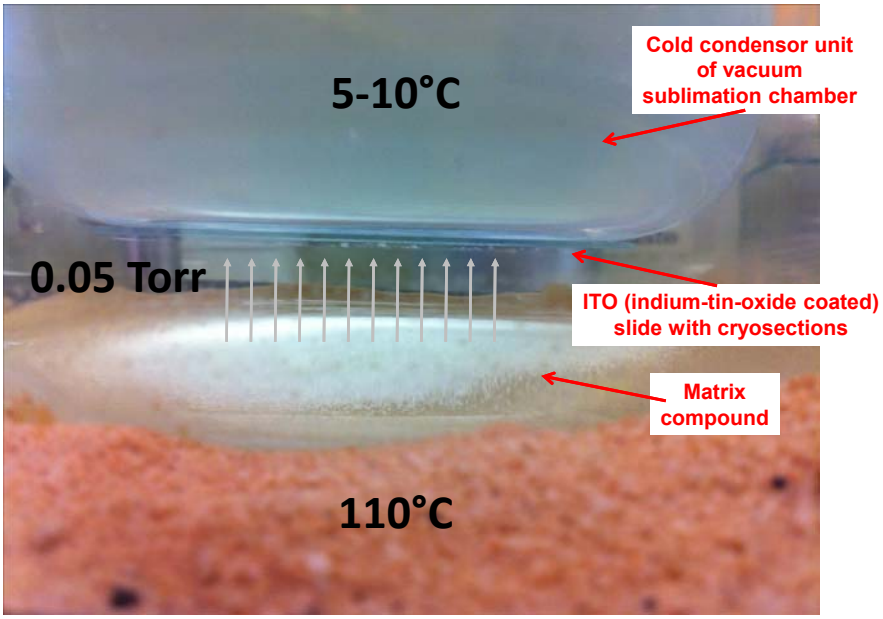

Slides with matrix applied by vacuum sublimation.

Deposition of the matrix compound is at the molecular level because gaseous molecules recrystallize at the relatively cold surface of the tissue section attached to the cold condenser.

The uniformity of matrix deposition onto the slide attached to the cold condenser surface reflects the random Brownian motion of the released gaseous matrix molecules.

Adapted MALDI plate holds slides for MALDI-IMS.

Conventional MALDI plate

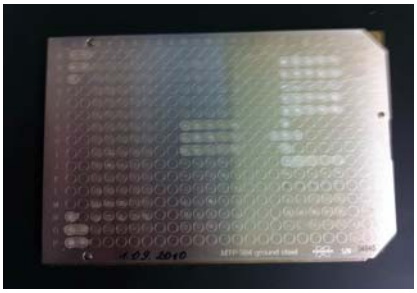

MALDI plate for cryosections

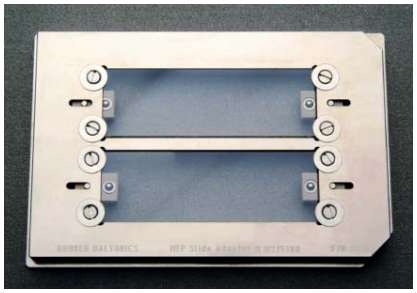

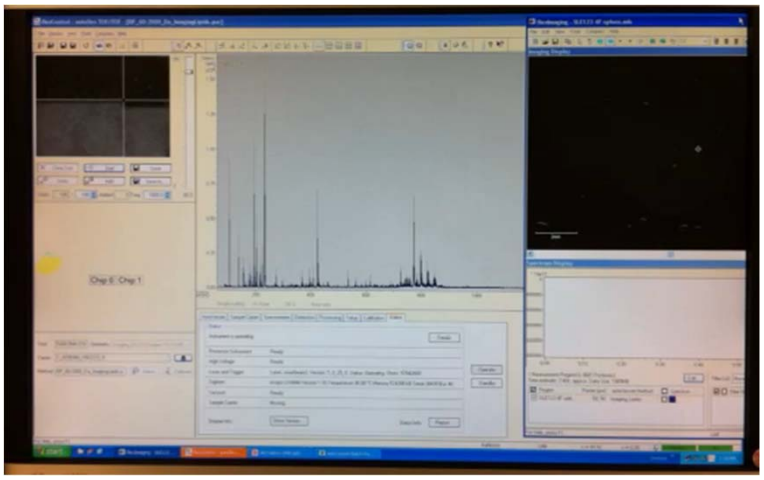

Quantitative and Spatial Analysis of Lipids in the aging eye lens.

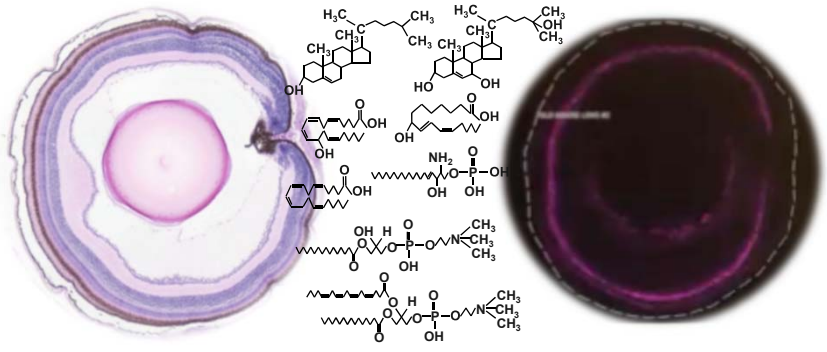

Specific aims of the study:

1) To characterize and compare the lens lipidomes of Mice and Zebrafish.
2) To analyze the changes that occur in the lens lipdome with aging.
3) To determine where lipid changes are occurring in the lens.

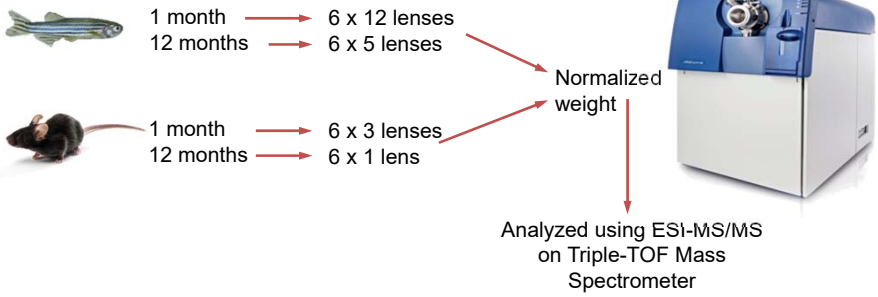

Stephen Barnes, Ph.D., Department of Pharmacology & Toxicology, Director UAB TMPL.

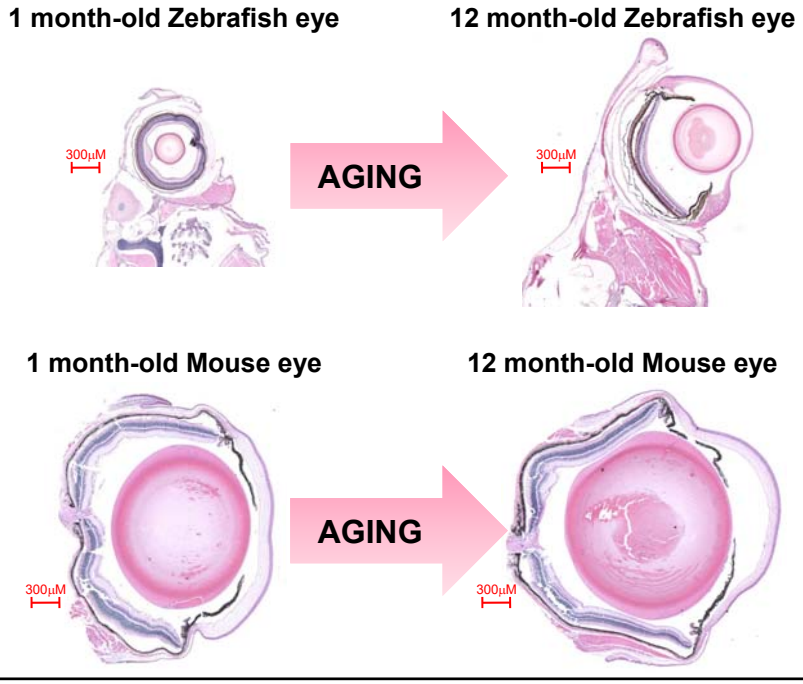

Mouse lens positive mode (Total lipids).

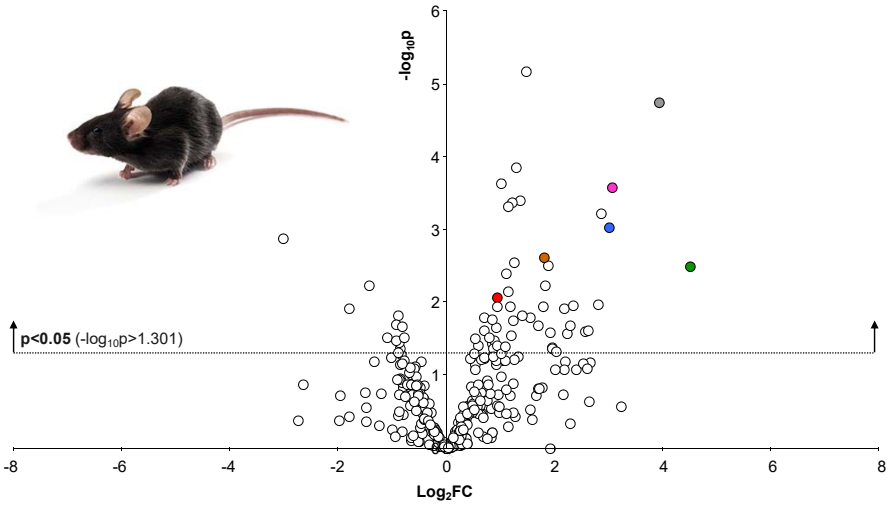

PC 36:4 (16:0/20:4) LPC 16:0 PC O-32:1 (PC) [ether lipid]

SM 32:3;4 SM 34:0;4 SM 34:1;3 (LCB 18:2, 2-2H2O, LCB 18:1;3-3H2O)

Zebrafish lens positive mode (Total lipids).

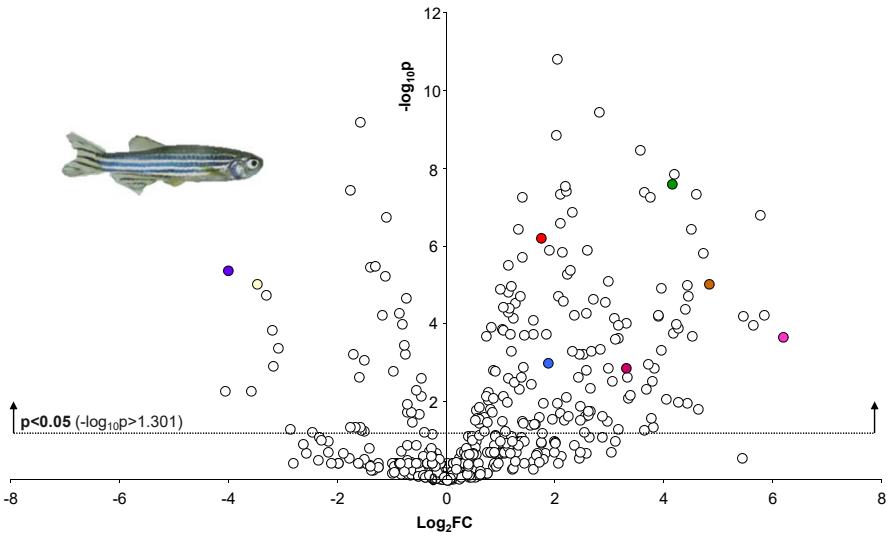

PC 36:4 (16:0/20:4) LPC 16:0 PE 36:0 MM(monomethyl) PE 36:0

SM 24:1;2 SM 32:3;4 SM 34:0;4 SM 34:1;3 (LCB 18:2, 2-2H2O, LCB 18:1;3-3H2O)

MS/MS fragments from782.6 m/z 36:4 PC (+mode).

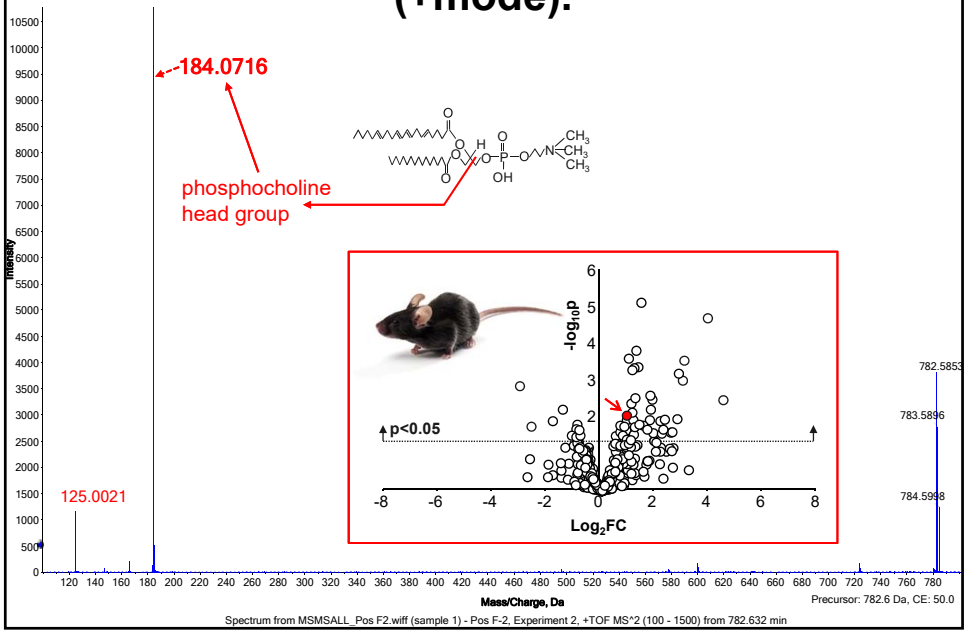

MS/MS fragments from 840.7 m/z 36:4 PC acetate adduct (-mode).

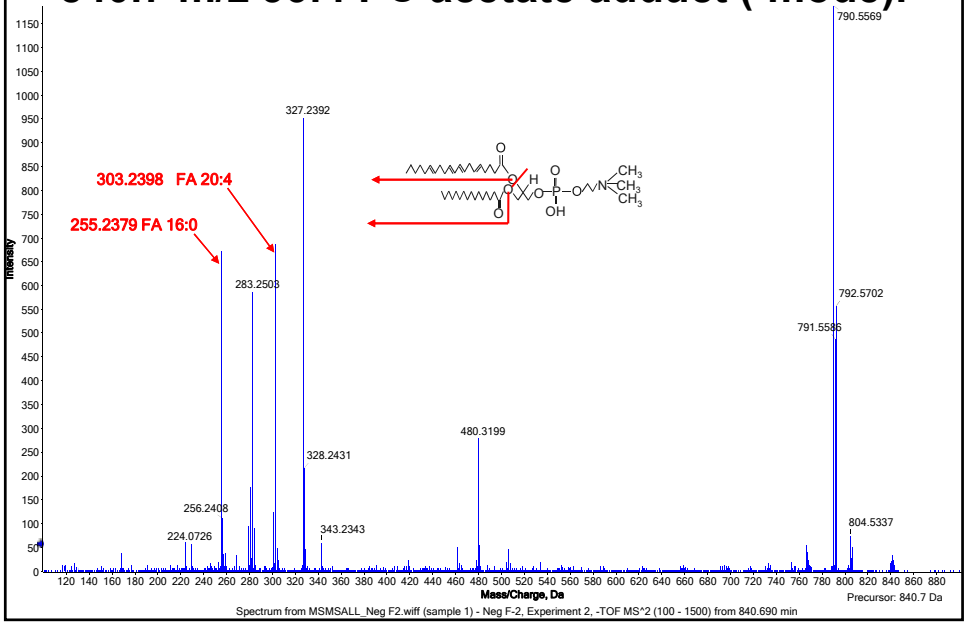

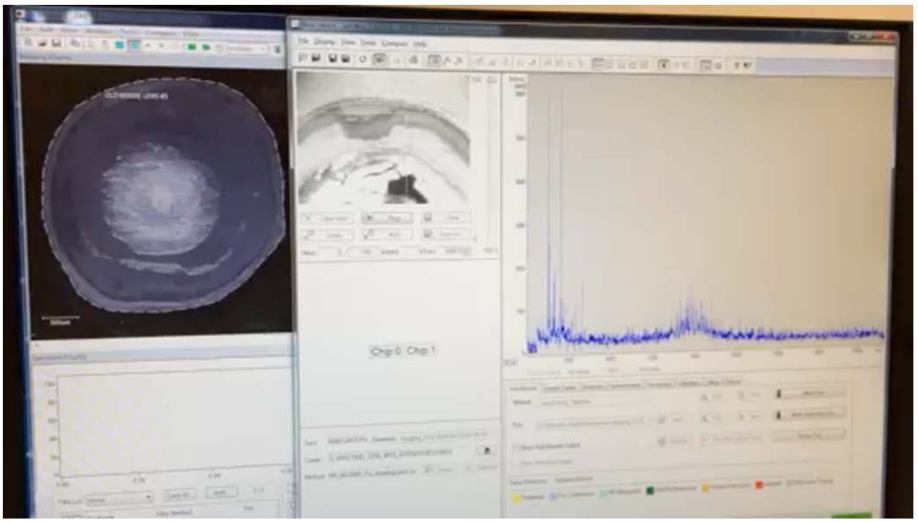

Spatial information on lens lipids provided by MALDI-Imaging MS.

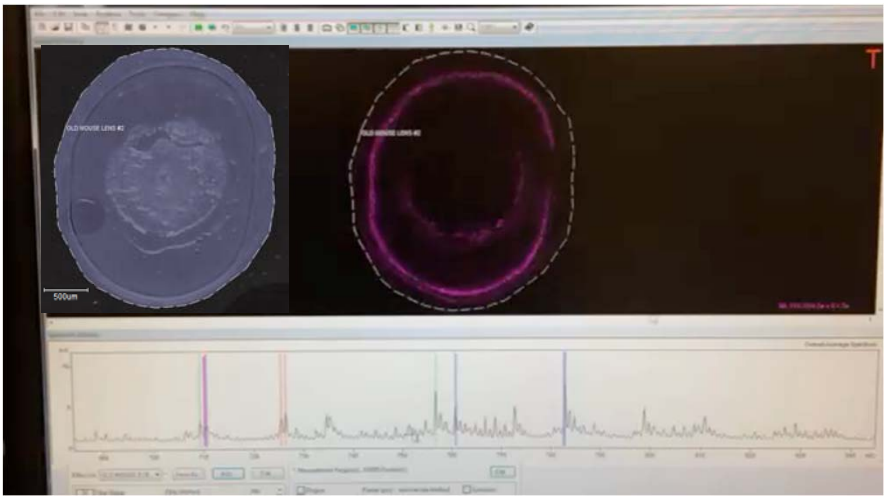

MALDI-IMS on 16:0/20:4 PC(36:4) in1 year old mouse eye.

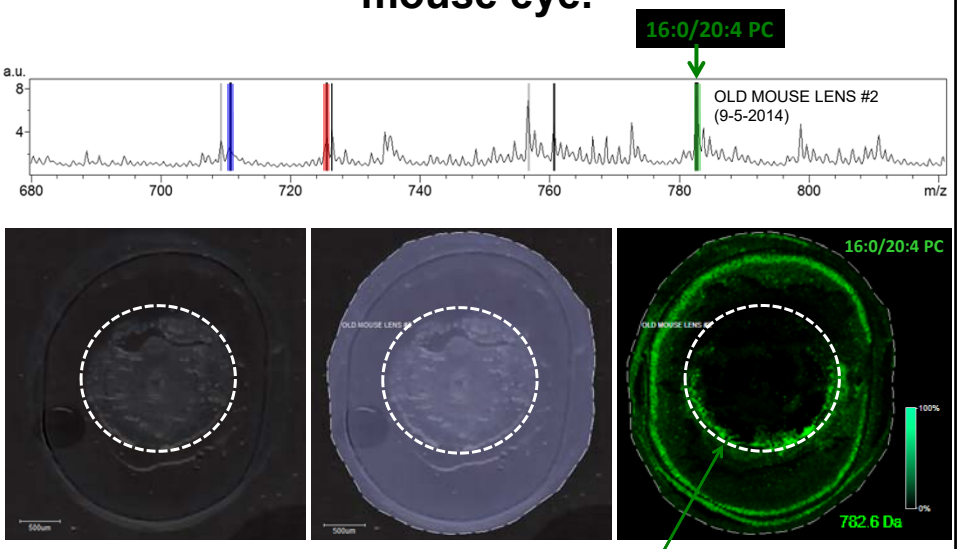

Lens 16:0/20:4 PC is localized exclusively to cortical region of the lens where metabolically active epithelial cells are present.

MS/MS of protonated PC(36:4) in eye using MALDI Imaging MS platform.

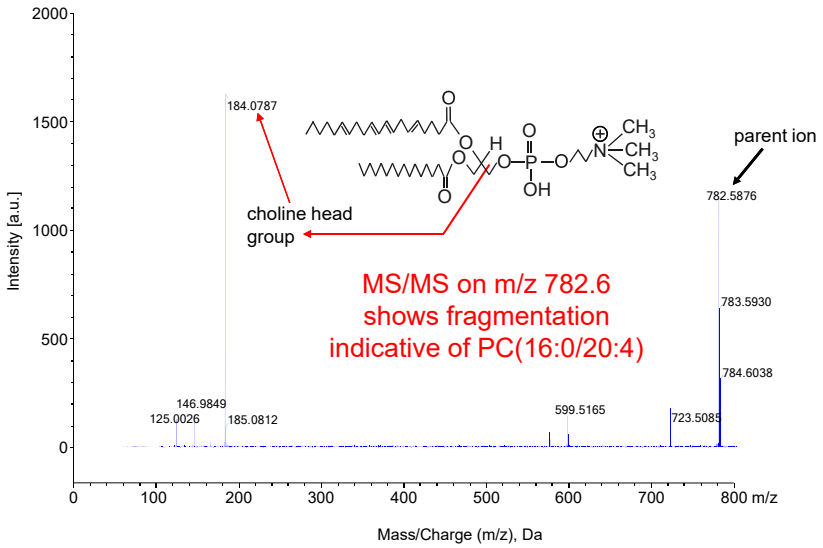

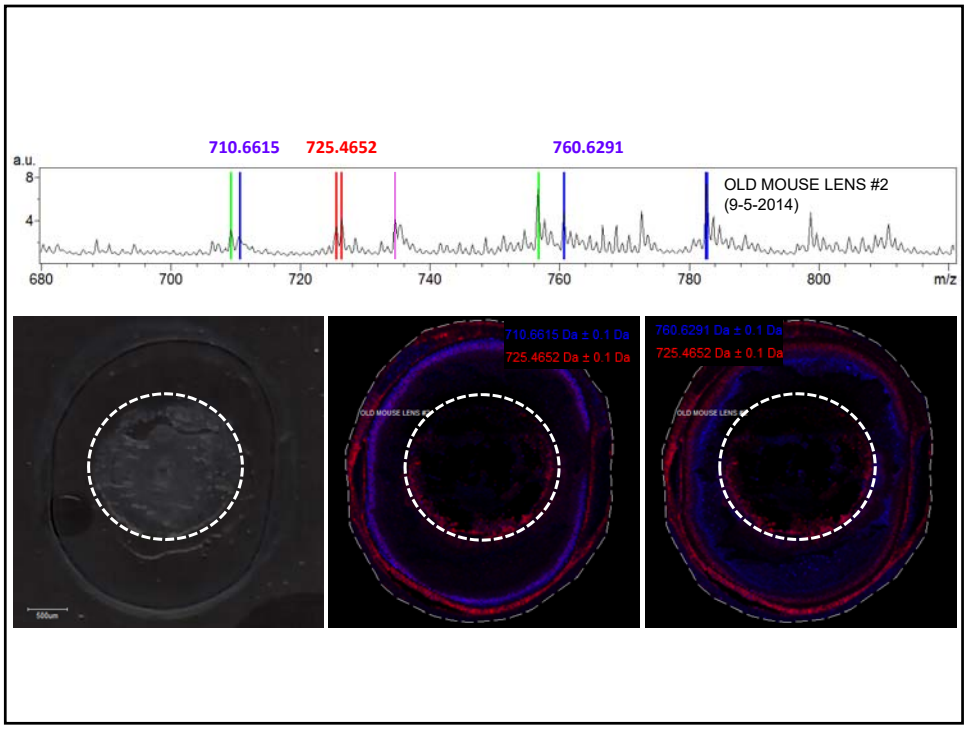
710.6615
725.4652
760.6291
a.u.
8
4
680
700
720
740
760
780
800
m/z
OLD MOUSE LENS #2
(9-5-2014)
710.6615 Da ± 0.1 Da
725.4652 Da ± 0.1 Da
760.6291 Da ± 0.1 Da
725.4652 Da ± 0.1 Da

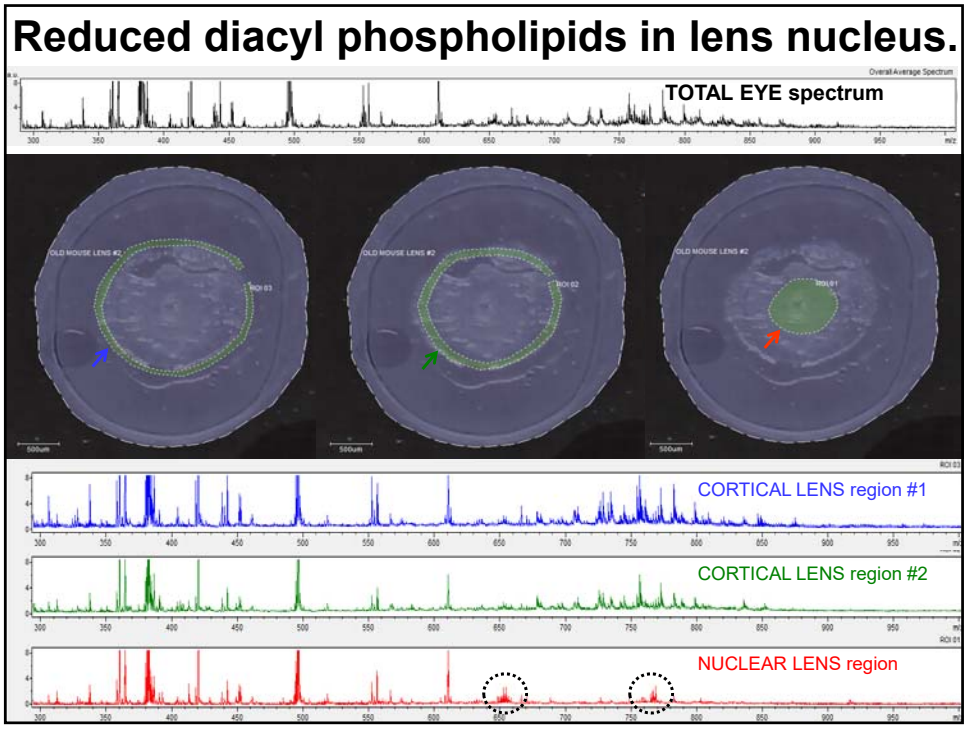
Reduced diacyl phospholipids in lens nucleus.
TOTAL EYE spectrum
CORTICAL LENS region #1
CORTICAL LENS region #2
NUCLEAR LENS region

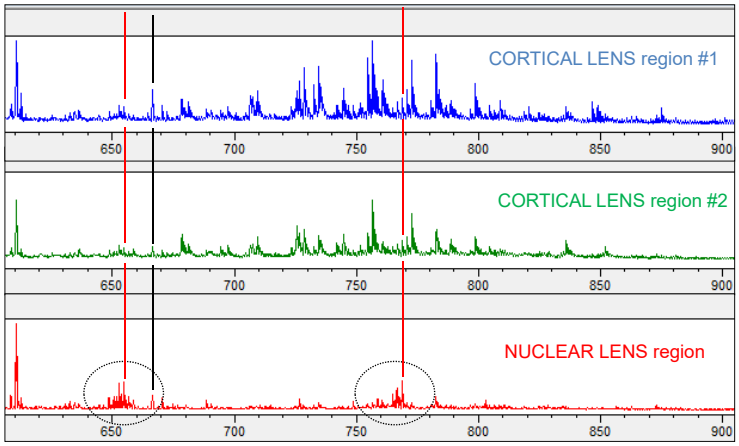

Quantitative and Spatial Analysis of Lipids Involved in Acute Kidney Injury.

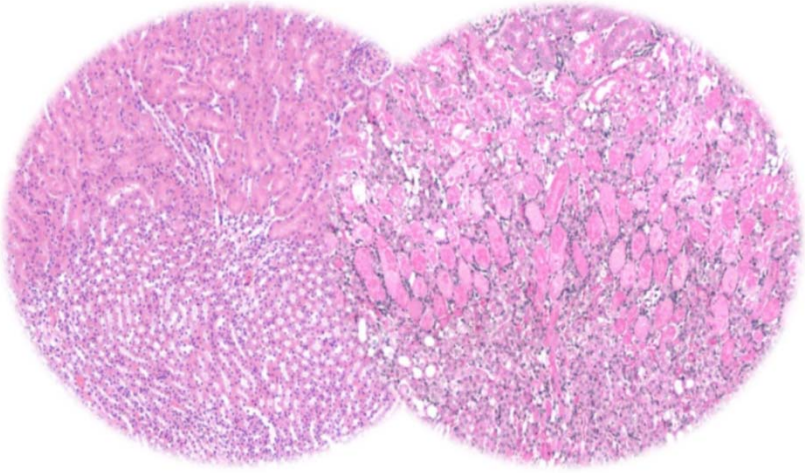

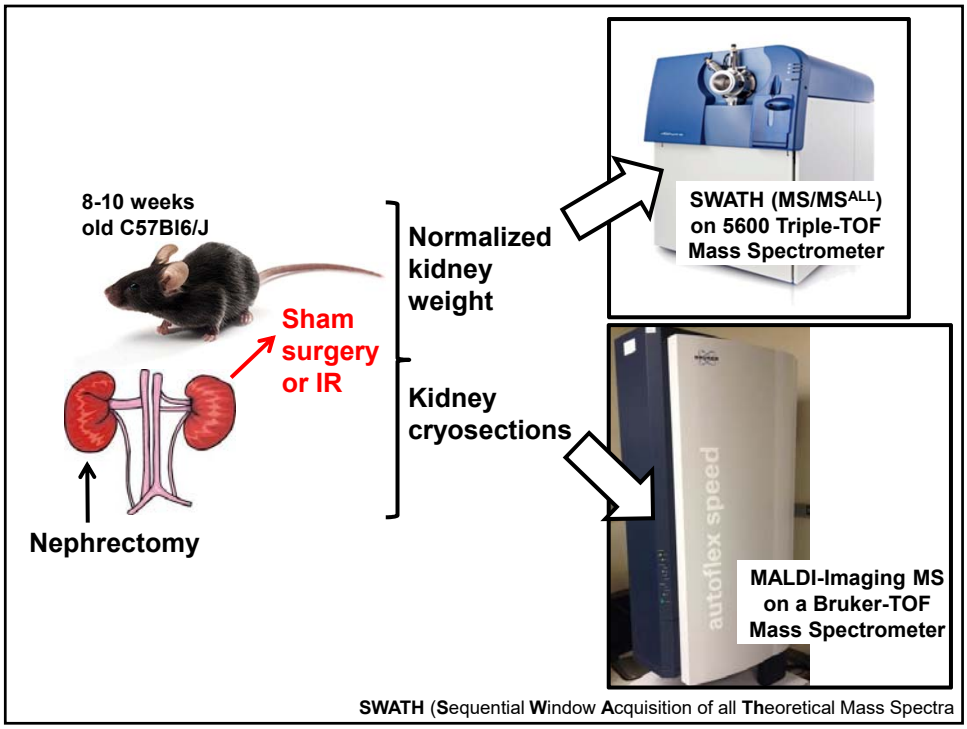

SWATH (**S**equential **W**indow **A**cquisition of all **Th**eoretical Mass Spectra

Plasma creatinine and kidney histology in mice subjected to ischemia/reperfusion (IR) related kidney injury at early and late time-points.

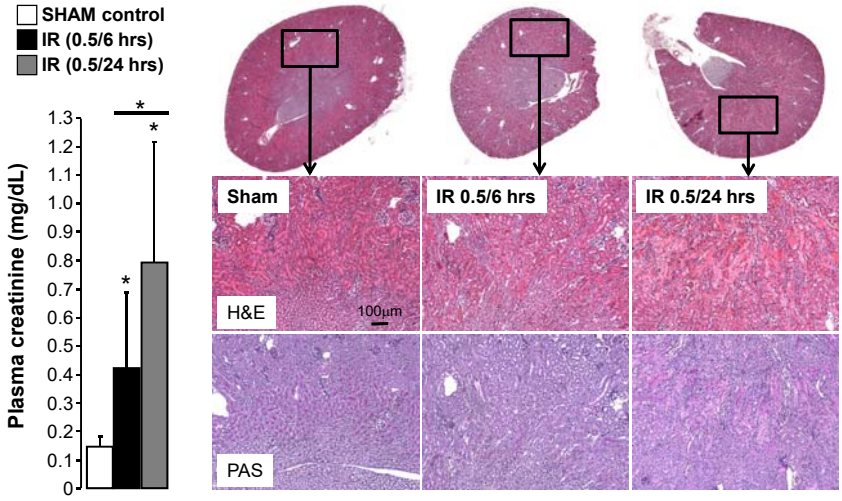

SWATH-MS on renal lipids following ischemia/reperfusion (IR)-related kidney injury

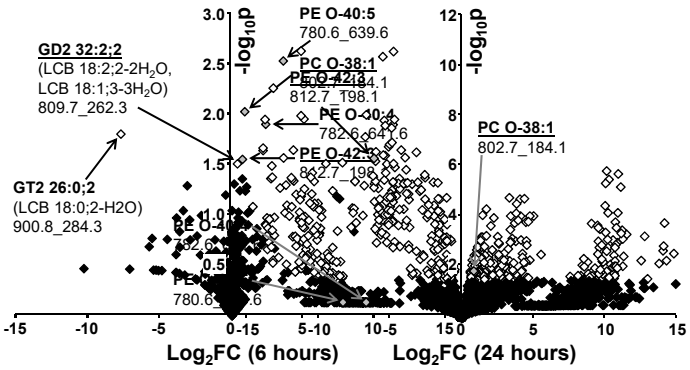

Early lipid changes in acute kidney injury using SWATH lipidomics coupled with MALDI tissue imaging. Rao S*, Walters KB*, Wilson L, Chen B, Bolisetty S, Graves D, Barnes S, Agarwal A, Kabarowski JH. Am J Physiol Renal Physiol, 310(10):F1136-47, 2016.

SWATH-MS on renal lipids following ischemia/reperfusion (IR)-related kidney injury

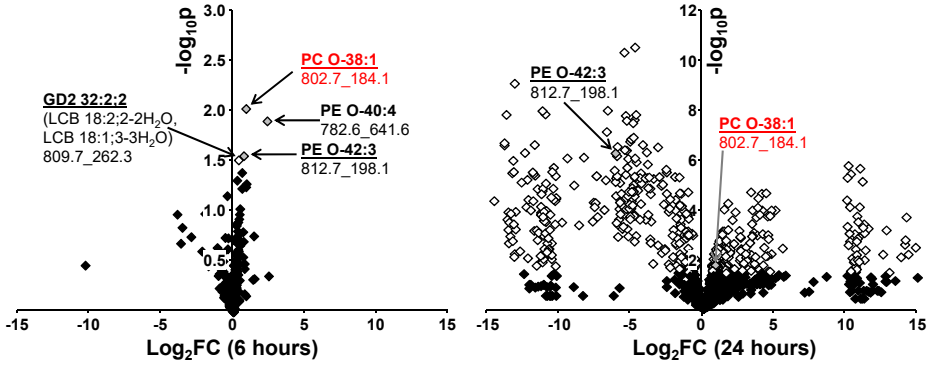

Intensity >10

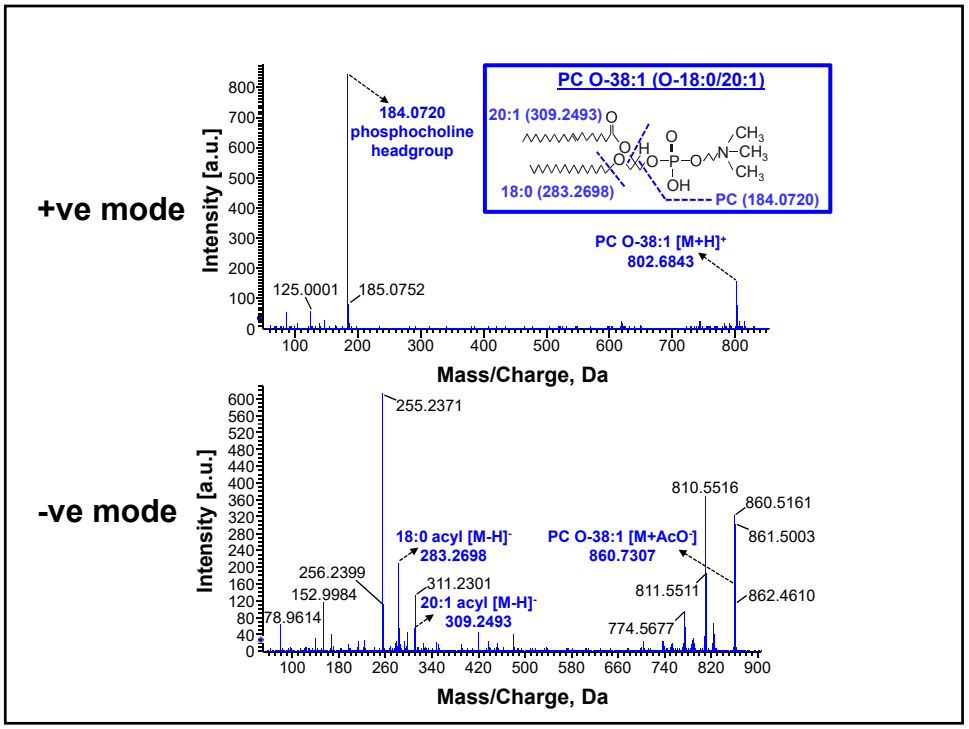
+ve mode
PC O-38:1 (O-18:0/20:1)
20:1 (309.2493)
18:0 (283.2698)
PC (184.0720)
184.0720
phosphocholine
headgroup
PC O-38:1 [M+H]+
802.6843
125.0001
185.0752
Intensity [a.u.]
Mass/Charge, Da
-ve mode
255.2371
810.5516
860.5161
861.5003
862.4610
18:0 acyl [M-H]-
283.2698
PC O-38:1 [M+AcO-]
860.7307
256.2399
152.9984
311.2301
20:1 acyl [M-H]-
309.2493
811.5511
78.9614
774.5677
Intensity [a.u.]
Mass/Charge, Da

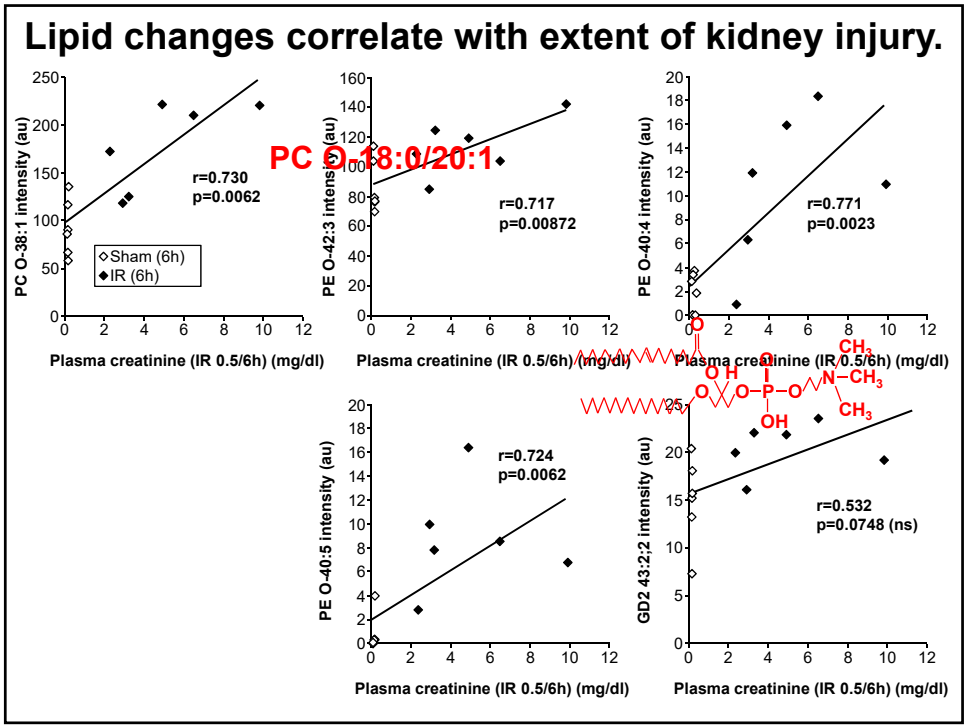
Lipid changes correlate with extent of kidney injury.
PC O-38:1 intensity (au)
r=0.730
p=0.0062
Sham (6h)
IR (6h)
Plasma creatinine (IR 0.5/6h) (mg/dl)
PC O-18:0/20:1
PE O-42:3 intensity (au)
r=0.717
p=0.00872
Plasma creatinine (IR 0.5/6h) (mg/dl)
PE O-40:4 intensity (au)
r=0.771
p=0.0023
Plasma creatinine (IR 0.5/6h) (mg/dl)
PE O-40:5 intensity (au)
r=0.724
p=0.0062
Plasma creatinine (IR 0.5/6h) (mg/dl)
GD2 43:2;2 intensity (au)
r=0.532
p=0.0748 (ns)
Plasma creatinine (IR 0.5/6h) (mg/dl)

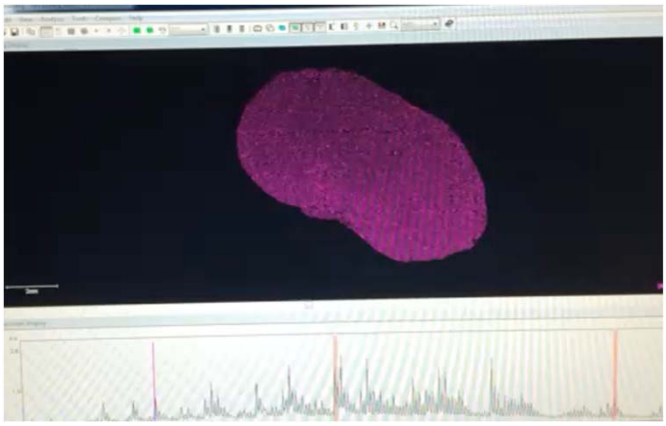

PC O-18:0/20:1 imaging in sham and IR kidneys.

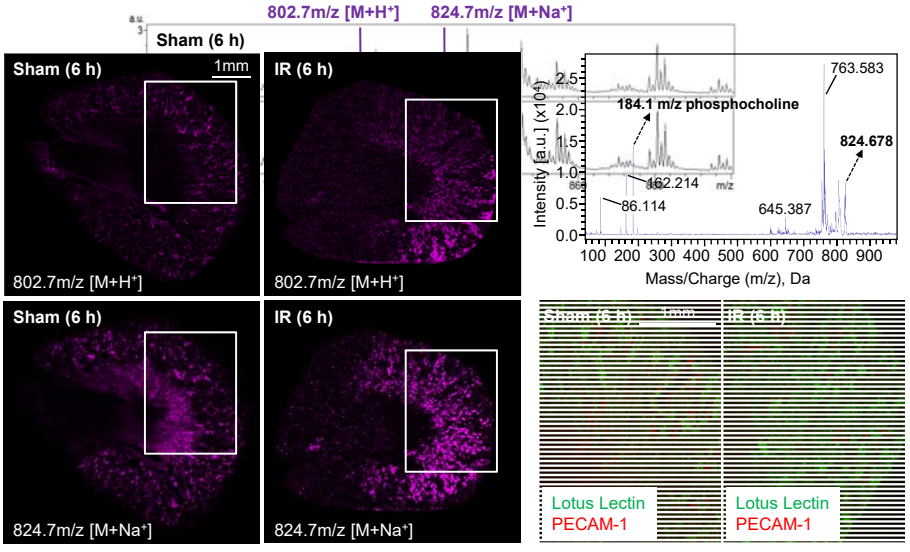

Rate-limiting peroxisomal enzymes in ether lipid synthesis are most abundant in proximal tubules.

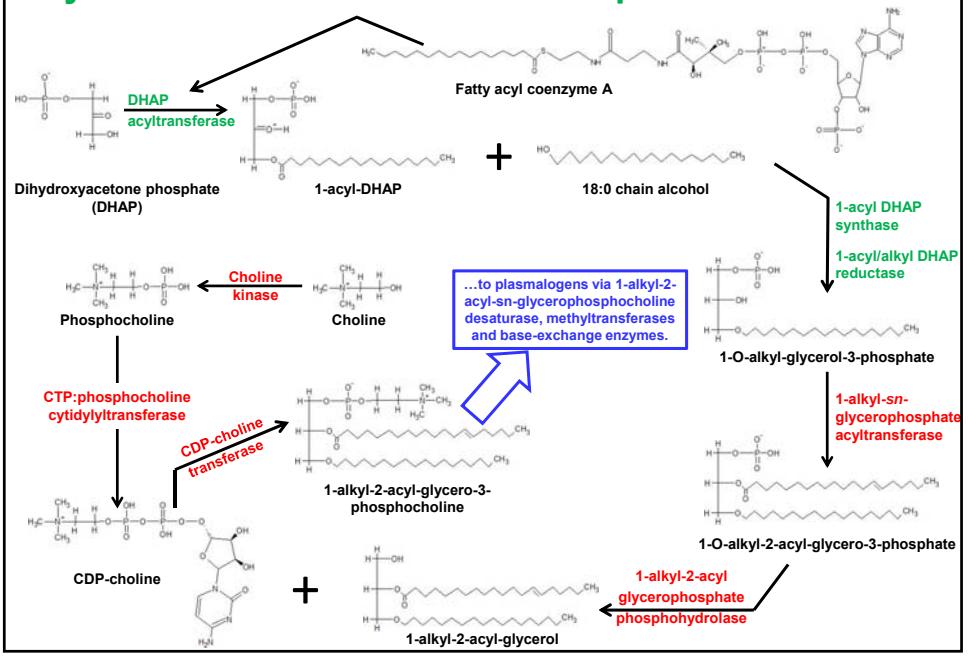

Other projects using SWATH lipidomics and MALDI-IMS.

Cosmic radiation effects on vascular inflammation and atherosclerosis risk (NASA).

New therapeutic lipoprotein mimetic peptides (NIH) (Drs. Roger White and Anantharamaiah, UAB).

Vascular Lipidomic Alterations in Mice Associated with Adhesive Effects of Heavy-Ion Space Radiation and Potential Consequences for Radiation-induced Atherosclerosis.

^{56}Fe radiation accelerates the development of atherosclerotic plaques in hyperlipidemic ApoE knockout mice.

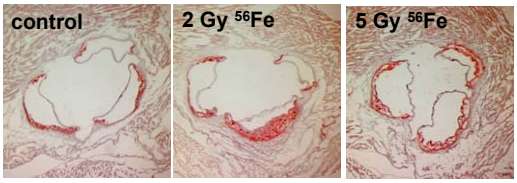

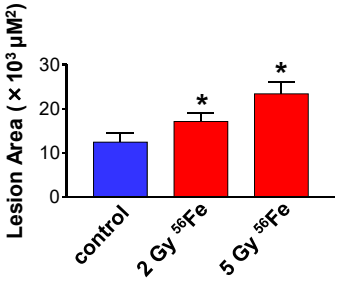

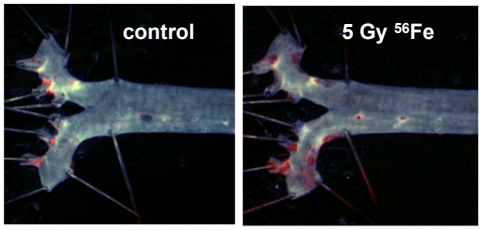

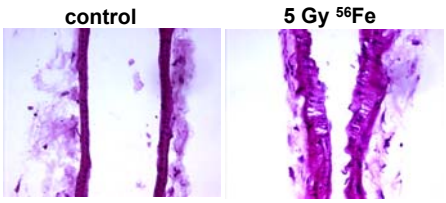

Ex vivo monocyte adhesion assay.

2-6 weeks

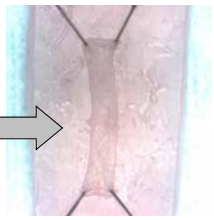

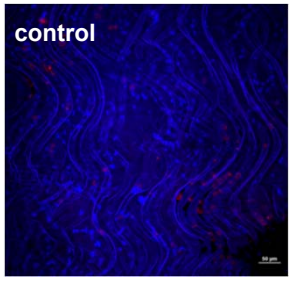

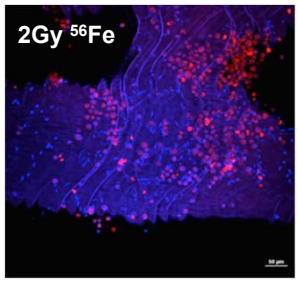

***En face* exposed aorta incubated with 4 x 10^6 fluorescent (CMTPX-labelled) WEHI-274.1 monocytes (30 minutes).**

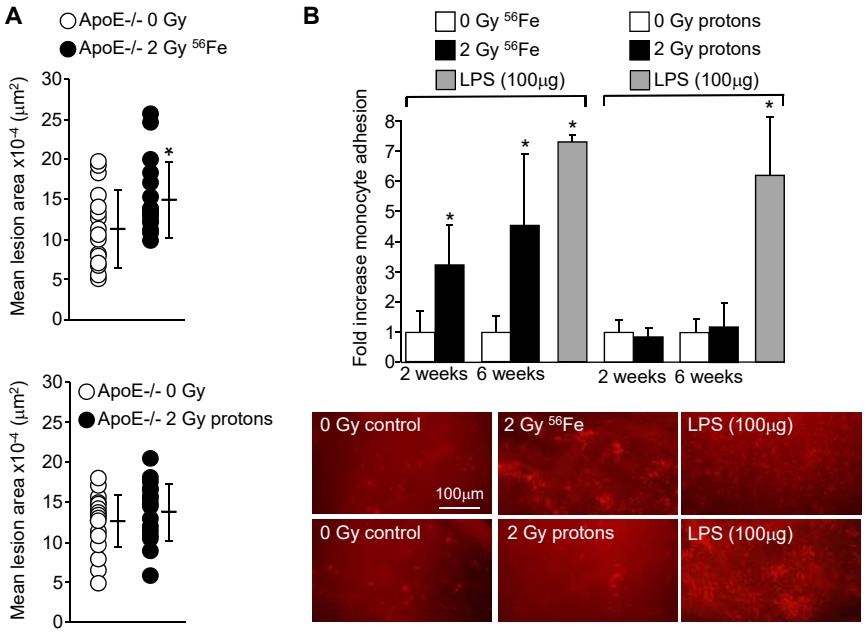

Exposure of C57BL/6J mice to space relevant doses of ^{56}Fe radiation increases adhesivity of aorta to monocytes.

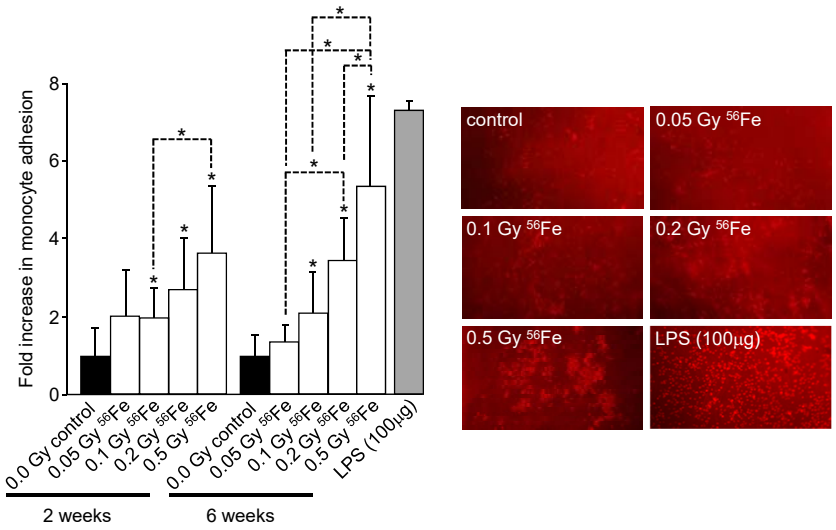

Early aortic lipid changes following exposure of normal mice to space relevant doses of ^{56}Fe radiation.

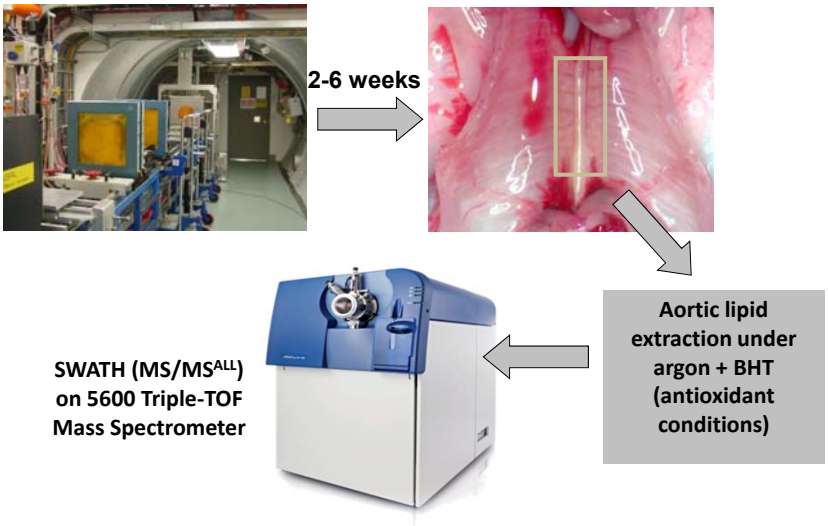

Early aortic lipid changes following exposure of normal mice to space relevant doses of ^{56}Fe radiation.

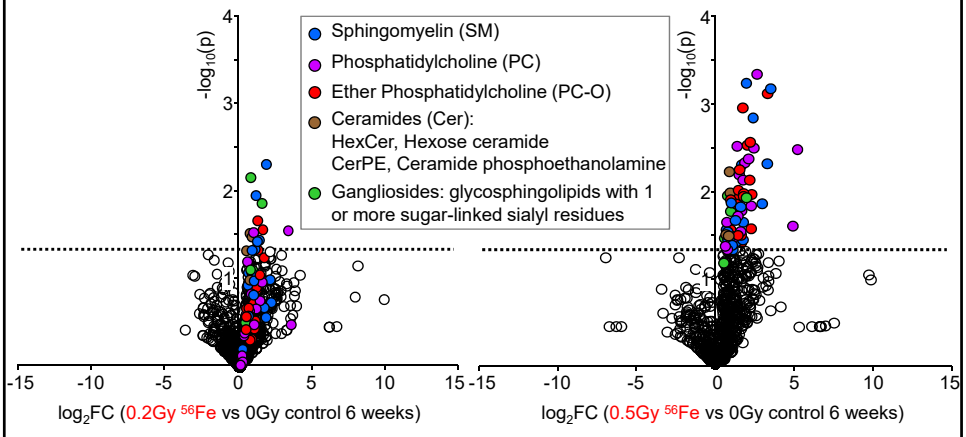

Lipoprotein-mediated entry and efflux of arterial lipids.

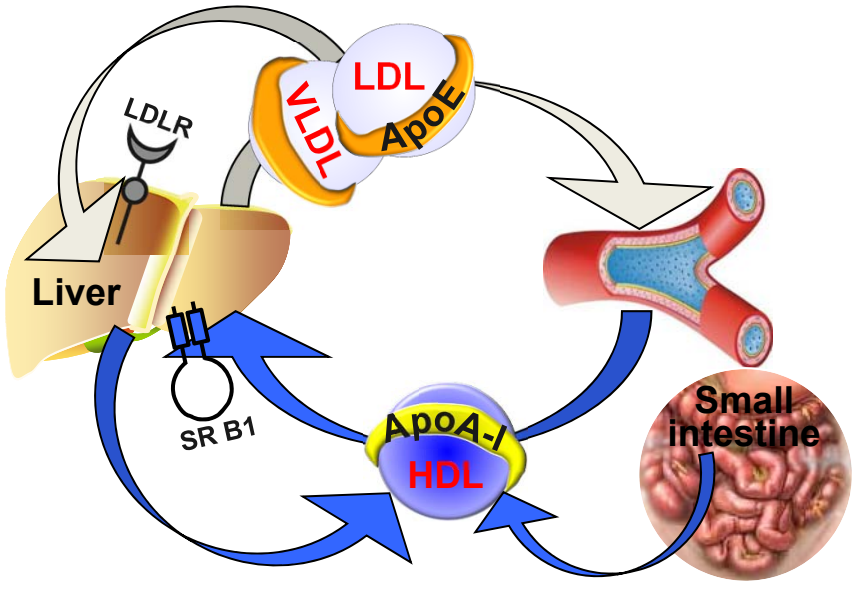

Changes in aortic lipids 6 weeks following ^{56}Fe exposure are not due to changes in lipid transport mechanisms related to HDL.

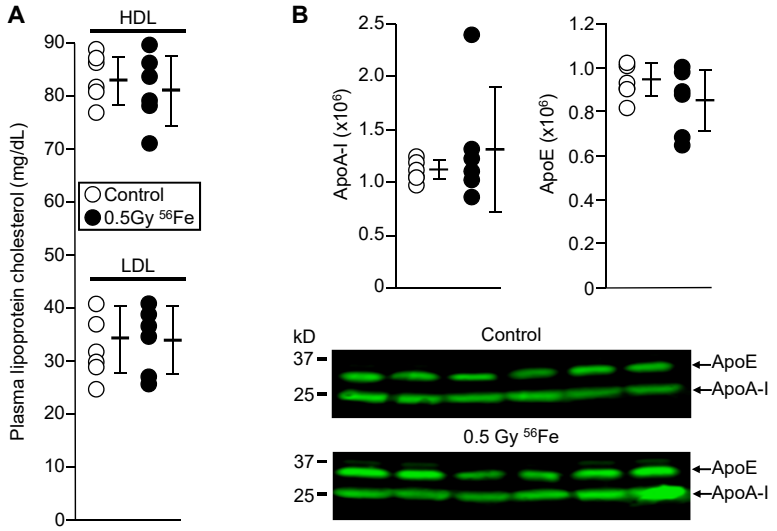

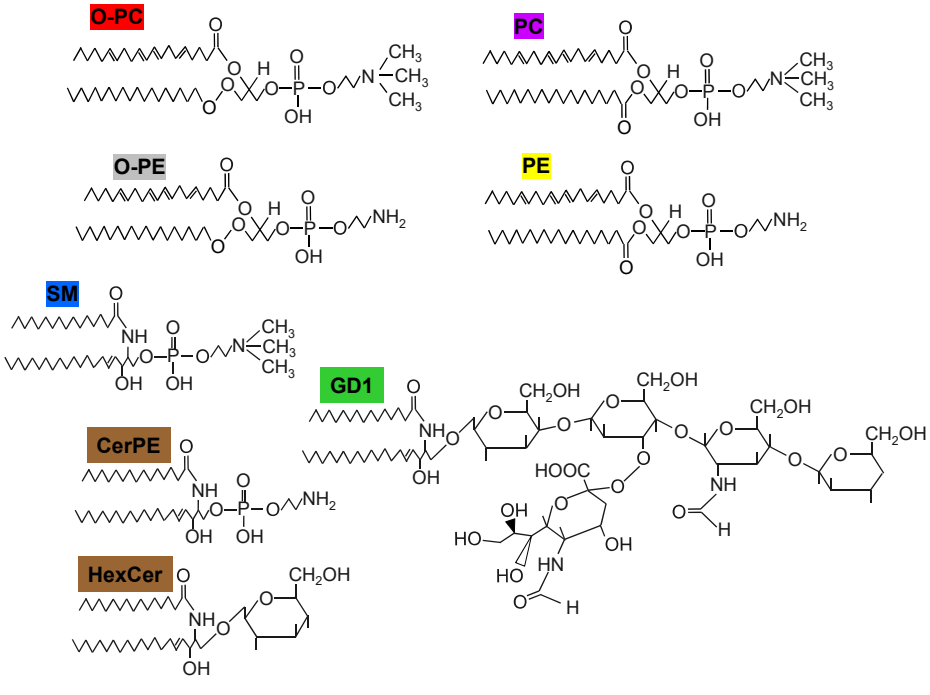

Imaging Mass Spectrometry for spatio-temporal analysis of vascular lipids.

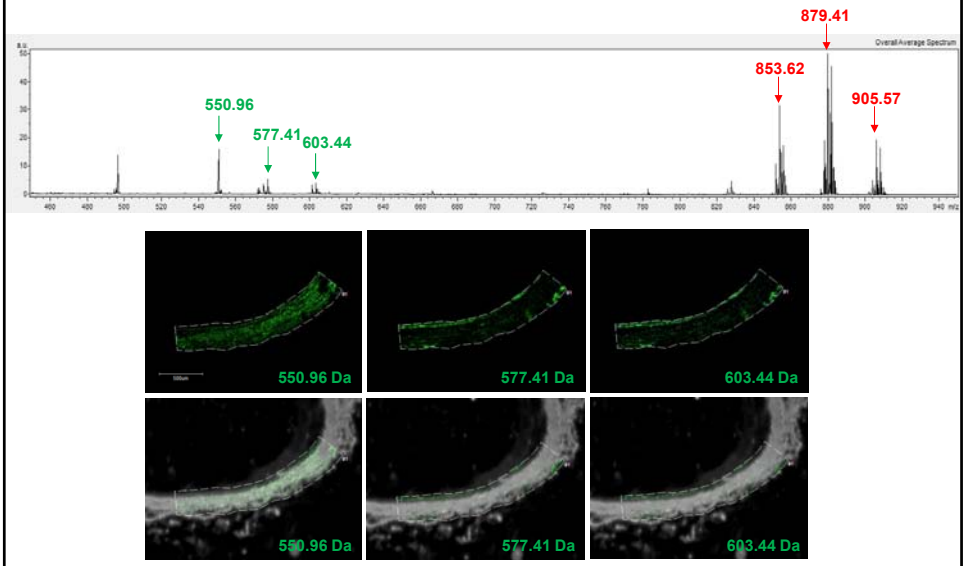

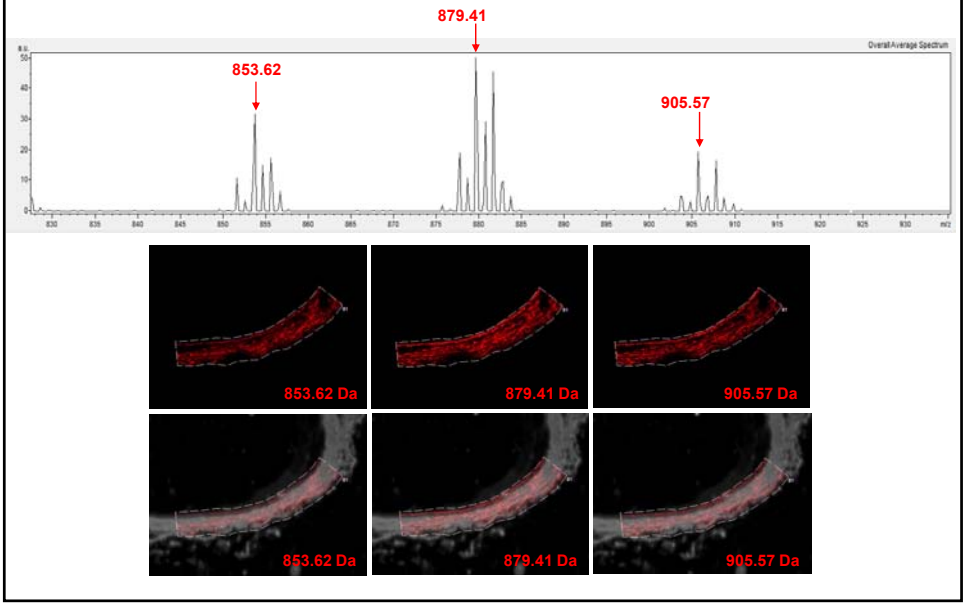

MS/MS fragmentation during MALDI imaging reveals phosphatidylcholine signature.

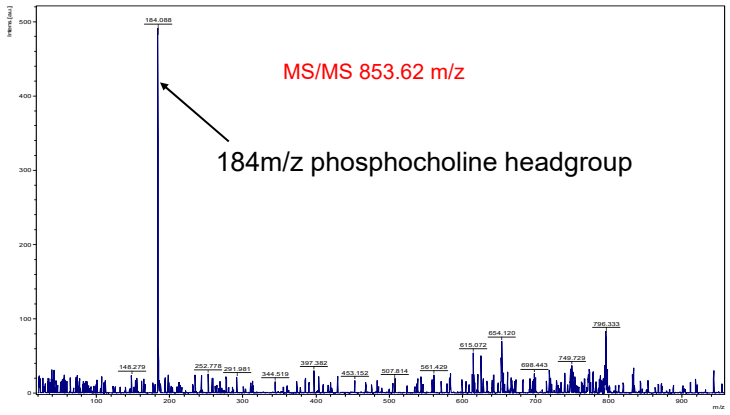

Distinct localization of lipids in the rabbit aorta.

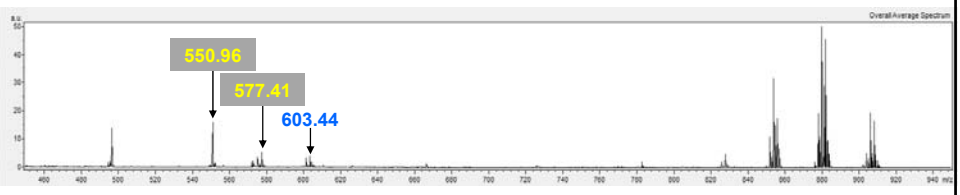

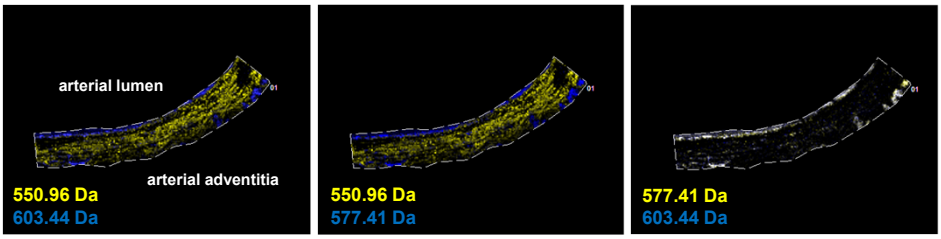

Kelly B. Walters
Miranda Collier
Kiran B. Gupta
UAB, Dept of Microbiology

Stephen Barnes
Landon Wilson
UAB, Targeted Metabolomics and Proteomics Lab

Dennis Kucik
UAB, Dept of Pathology

Anupam Agarwal
Sangeetha Rao
UAB, Dept of Medicine and UAB/UCSD O'Brien Center for Acute Kidney Injury Research